A DNA binding winged helix domain in CAF-1 functions with PCNA to stabilize CAF-1 at replication forks

Kuo Zhang[1,2,†], Yuan Gao[3,†], Jingjing Li[1,†], Rebecca Burgess[3], Junhong Han[4], Huanhuan Liang[1], Zhiguo Zhang[3,*] and Yingfang Liu[1,*]

[1]State Key Laboratory of Biomacromolecules, Institute of Biophysics, Chinese Academy of Sciences, 15 Datun Road, Chaoyang District, Beijing 100101, China, [2]University of the Chinese Academy of Sciences, Beijing 100049, China, [3]Department of Biochemistry and Molecular Biology, Mayo Clinic, Rochester, MN 55905, USA and [4]State Key Laboratory of Biotherapy and Cancer Center, Division of Abdominal Cancer, West China Hospital, Sichuan University, and National Collaborative innovation Center for Biotherapy, Chengdu 610041, China

ABSTRACT

Chromatin assembly factor 1 (CAF-1) is a histone H3–H4 chaperone that deposits newly synthesized histone (H3–H4)$_2$ tetramers during replication-coupled nucleosome assembly. However, how CAF-1 functions in this process is not yet well understood. Here, we report the crystal structure of C terminus of Cac1 (Cac1C), a subunit of yeast CAF-1, and the function of this domain in stabilizing CAF-1 at replication forks. We show that Cac1C forms a winged helix domain (WHD) and binds DNA in a sequence-independent manner. Mutations in Cac1C that abolish DNA binding result in defects in transcriptional silencing and increased sensitivity to DNA damaging agents, and these defects are exacerbated when combined with Cac1 mutations deficient in PCNA binding. Similar phenotypes are observed for corresponding mutations in mouse CAF-1. These results reveal a mechanism conserved in eukaryotic cells whereby the ability of CAF-1 to bind DNA is important for its association with the DNA replication forks and subsequent nucleosome assembly.

INTRODUCTION

The proper development of multicellular organisms depends on the distinct specification of different cell types. Despite having identical genomes, cells display distinct gene expression patterns and phenotypes, which can persist after numerous cell divisions (1). Cell identity is maintained, in part, through epigenetic mechanisms. However, the process by which epigenetic states of chromatin are propagated to daughter cells during mitotic cell division (also known as epigenetic inheritance) is one of the challenging questions in the field of epigenetics. One key process that contributes to epigenetic inheritance is the assembly of the nucleosome, the basic repeating unit of chromatin. The nucleosome consists of 145–147 base pairs of DNA wrapped around a histone octamer containing one histone (H3–H4)$_2$ tetramer and two histone H2A–H2B dimmers (2–4). Nucleosomes act as a barrier to any DNA-related process (such as DNA replication, transcription and repair), therefore they need to be disassembled so that the machinery can have access to the DNA strands (5). Following DNA replication during S phase, nucleosomes are reassembled using both parental histones and newly synthesized histones in a process called replication-coupled nucleosome assembly (6). By virtue of their high basic charge, histones and DNA tend to form insoluble aggregates when directly mixed in physiological conditions. To prevent these deleterious effects, a network of histone chaperones are responsible for binding and delivering histones to DNA to form nucleosomes during DNA replication, repair as well as transcription (7–9).

In general, histone chaperones can be classified as either H3–H4 or H2A–H2B chaperones based on their preferential binding to H3–H4 or H2A–H2B. Chromatin assembly factor 1 (CAF-1) is a H3–H4 chaperone, which was first discovered in human cells for its ability to assemble replicating DNA into nucleosomes using newly synthesized histone H3–H4 (6,10). CAF-1 is a three-subunit complex conserved in eukaryotic organisms. In S. cerevisiae, CAF-1 consists of Cac1, Cac2 and Cac3. CAF-1 has evolutionarily conserved functions in DNA replication, repair and heterochromatin silencing (11–16). Recent studies have suggested that CAF-

*To whom correspondence should be addressed. Tel: +86 1064888536; Fax: +86 1064888536; Email: liuy@ibp.ac.cn
Correspondence may also be addressed to Zhiguo Zhang. Tel: +1 507 538 6074; Fax: +1 507 284 3383; Email: zhang.zhiguo@mayo.edu
†These authors contributed equally to the paper as first authors.

1 is also involved in developmental pathways, epigenetic memories and asymmetric cell division (17–20).

Newly synthesized H3–H4 complexes initially form hetero-complex with the histone chaperone anti-silencing factor 1 (Asf1) (Asf1-H3–H4), which will serve as the ideal substrate for the acetylation of H3K56 (H3K56ac) by the histone acetyltransferase Rtt109-Vps75 complex in S. cerevisiae (21). H3K56ac then promotes the ubiquitylation of H3K121, K122 and K125 by Rtt101-MMS1 (22). This ubiquitylation weakens the interaction between Asf1 and H3–H4, which will then facilitate the hand-off of H3–H4 to CAF-1 and another chaperone Rtt106. CAF-1 and Rtt106 then assemble H3–H4 tetramers for nucleosome formation (23–25).

Studies in yeast and human cells indicate that the ability of CAF-1 to preferentially assemble replicating DNA into nucleosomes depends, at least in part, on its ability to interact with proliferating cell nuclear antigen (PCNA). PCNA is associated with replicated DNA molecules and attracts CAF-1 to the site of DNA replication (26–29). In S.cerevisiae, disruption of CAF-1-PCNA interaction impairs the role of CAF-1 in telomere silencing and silent mating-type locus, HMR, but interestingly, causes only partial loss of function compared with Cac1 deletion (26,29,30). Thus, there might be other factors existing to promote CAF-1's ability to assemble replicating DNA into nucleosomes.

We attempted to study the structure of yeast CAF-1. During this process, we identified an independent domain at the C terminal of Cac1 subunit (termed as Cac1C). The structure of this domain was then determined by crystallographic method. Unexpectedly, we found that Cac1C bears a winged helix domain (WHD) structure. Electrophoretic mobility shift assay (EMSA) reveals that this domain binds to DNA without sequence specificity. Mutagenesis analysis shows that the DNA-binding ability of WHD motif in CAF-1, functioning with PCNA, helps to recruit and stabilize CAF-1 at the replication forks in yeast and mouse cells. Therefore, our studies reveal a conserved mechanism whereby CAF-1 functions in DNA replication-coupled nucleosome assembly.

MATERIALS AND METHODS

Protein expression and purification

Cac1C was expressed as a glutathione S-transferase (GST) fusion protein in *Escherichia coli*. The GST tag was removed by protease cleavage, and Cac1C was purified by successive chromatographic methods. The CAF-1 complex was expressed in baculovirus-infected sf9 insect cells. *Cac1* (residues 91–606aa) and the full-length *Cac3* genes were fused with the *MBP* gene from the pMAL-C2P vector (Invitrogen) at the N-terminal and ligated by a PreScission Protease cleavage site. The fused genes were cloned into the pFastBac-1 vector (Invitrogen). The *Cac2* (residues 1–438) gene was cloned into the pFastBac-1 vector directly and expressed in sf9 insect cells. The MBP tag was removed by protease cleavage using PreScission Protease, and CAF-1 was purified by successive chromatographic methods. Details of the methods are described in Supplementary materials and methods.

Yeast strains and plasmids

All yeast strains used in our experiments were derived from W303 (leu2–3, 112 ura3–1 his3–11, trp1–1, ade2–1, can1–100). Standard yeast media and manipulations were used. Cac1 expression plasmids were constructed using standard methods and the pRS313vector. Green Fluorescent Protein labeled p150 (GFP-p150) wild type (WT) and the mutants were expressed using a lentivirus-based vector. Oligos used to construct the Cac1 and p150 mutants are listed in Supplementary Table S1.

Crystallization and structure determination

Cac1C crystals were obtained in a solution containing 0.1 M NaCl, 1.5 M (NH4)$_2$SO$_4$ and 0.1 M BIS-Tris (pH 6.5) and were flash-frozen in 20% glycerol as a cryoprotectant. Anomalous diffraction data at a resolution of 2.75 Å using selenomethionine (Se)-derivative crystals was collected at the Shanghai synchrotron radiation facility beamline BL17U (SSRF, China; λ = 0.979 Å). The data were processed using HKL2000 (31). Phasing was performed using the single-wavelength anomalous dispersion (SAD) method with the Se-derivative data by SHELX (32) and was improved by PHENIX AutoSol (33). Automatic protein model building was performed with PHENIX Auto-Build (33). The resulting protein models were completed manually using COOT (34). The final model was refined using REFMAC1 (35), and its stereochemical quality was checked using PROCHECK (36). In the Ramachandran plot, 93.5% of the amino acids in the final atomic model were in the most favorable region and 6.5% were in the additional allowed region. Structural figures were prepared using PyMOL (www.pymol.org).

EMSA

All the oligonucleotides used in this study were synthesized by Sangon (Shanghai, China). Two strands of complementary single-stranded DNA (ssDNA) were annealed to form dsDNA. 5-Carboxyfluorescein (5-FAM) labeled DNA was mixed with the indicated quantity of protein in a buffer (20 mM Tris pH 7.5, 100 mM NaCl and 1 mM DTT). The reaction mixture was incubated on ice for 1 h and analyzed by electrophoresis in native PAGE at 100 V using 0.5x TBE buffer on ice. The gels were scanned with Typhoon Troi + (GE Healthcare). To compare the binding affinities, the integrated density value of each band was quantified by ImageJ (1.46r). The data were analyzed by non-linear regression equation using the Graph Pad Prism software and fitted one site-specific binding model.

DNA binding assay

The biotinylated 58 bp oligonucleotide was synthesized by Sangon (Shanghai, China). Two strands (one was biotinylated) of complementary ssDNA were annealed to form dsDNA. Streptavidin Sepharose beads (GE Healthcare) were incubated with 58 bp of biotinylated dsDNA in buffer (20 mM Tris pH 7.5, 150 mM NaCl, 0.01% NP40, 10% glycerol and 1 mM DTT) at 4°C for 30 min. The beads were washed three times with the same buffer to remove the excess DNA.

Equal beads labeled with DNA were further incubated with indicated amount of purified proteins at 4°C for an additional 30 min. The beads were washed three times, analyzed by SDS-PAGE and detected with Coomassie Blue staining or immunoblotting with a GST antibody (TIANGEN, 1:2000).

Histone binding assay

Histones H3 and H4 were prepared as described previously (37). Histones H3 and H4 from *Xenopus laevis* were overexpressed in *E. coli* strain BL21 (DE3) cells, purified separately under denaturing conditions and combined to reconstitute the (H3–H4)$_2$ tetramer.

In GST pull-down experiments, the purified GST-tagged Cac1C and CAF-1 (WT or mutants) were immobilized on 50 μl glutathione resin. The beads were incubated with excess histone H3–H4 in buffer (20 mM Tris pH 7.5, 300 (or 200) mM NaCl, 0.01% NP40, 10% glycerol and 1 mM DTT) at 4°C for 1 h. The beads were washed three times with the same buffer, analyzed by SDS-PAGE and detected with Coomassie Blue staining.

PCNA binding assay

Purified PCNA with his tag at the C-terminal (PCNA-his) was mixed with GST-tagged protein in buffer (20 mM Tris pH 7.5, 100 mM NaCl and 0.01% NP40). The mixture was further incubated with 20 μl glutathione resin at 4°C for 1 h. The beads were washed three times with the same buffer and analyzed by SDS-PAGE. PCNA-his was detected by immunoblotting with his antibody (TIANGEN, 1:2000). The GST-tagged proteins were detected by Coomassie Blue staining or immunoblotting with GST antibody (TIANGEN, 1:2000).

Silencing assays

Assays for silencing at the *HMR* locus were performed as described in cells containing a GFP reporter integrated at the silent *HMR* locus (38). Cells grown at 25°C to an optical density at 600 nm value of 0.6–0.8 were washed three times with synthetic complete-TRP media. The percentage of cells expressing GFP was determined using flow-assisted cell sorting (FACS) analysis.

Chromatin binding assay

Yeast cells were grown in 5 ml of selective medium at 25°C overnight. Each strain was diluted to 15 ml to OD$_{600}$ = 0.2 and grown until OD$_{600}$ ~0.8 at 25°C. A total of 0.5 ml of each culture was harvested for FACS analysis. The rest cells were collected and washed once with 1 ml of ice-cold 20% glycerol. The chromatin binding assay was performed as described (39). Proteins in chromatin and soluble fractions were analyzed by Western blot analysis using antibodies against Cac1 (40) (rabbit polyclonal, 1:2000), PCNA (871, 1:10000), Orc3 (SB3, 1:2000) and H3 (rabbit polyclonal, 1:1000).

Cell culture and fluorescence microscopy

Mouse NIH3T3 cells were plated on poly-L-lysine-coated glass coverslips and grown in Dulbecco's modified Eagle medium (DMEM) with 10% fetal bovine serum (FBS). We carried out pre-extraction of cells prior to fixation for 5 min with 0.2% Triton in phosphate buffered saline (PBS) buffer plus 1% goat serum on ice and fixed the cells in cold methanol for 20 min. The cells were permeabilized with 0.5% Triton X-100 in PBS buffer for 5 min at room temperature and then blocked with 5% goat serum in PBS buffer for at least 1 h. Primary antibodies at appropriate dilutions (α-PCNA:PC10,1:100; α-GFP:Ab6556,1:1000) were added to the cells and incubated at room temperature for at least 2 h. The cells were washed with PBS buffer twice and probed with FITC/Rhodamine-conjugated secondary antibodies at room temperature for 1 h. DNA was stained with DAPI, and the samples were mounted with Gold antifade reagents (Invitrogen) and examined using a Zeiss Axioplan Fluorescence microscope (100x objective).

RESULTS

Crystal structure of Cac1C

We solved the structure of yeast Cac1C (residues 520–606 aa) at a resolution of 2.75 Å by the SAD method using a Se-derivative protein crystal (Supplementary Table S2). Cac1C consisted of four helices, two antiparallel strands and a long wing loop (w1), arranged in the order of α1-α2-α3-β1-w1-β2-α4 (Figure 1A). We determined through Dali search (http://ekhidna.biocenter.helsinki.fi/dali_server) that Cac1C shared highly structural similarities with some WHD-containing proteins, such as human ATP-dependent DNA helicase RECQ1 (41) (Figure 1B), human transcriptional activator regulatory factor RFX1 (42) (Figure 1C), E2F transcription factor 4 (E2F4) (43) (Supplementary Figure S1A) and human RecQ helicase WRN (44) (Supplementary Figure S1B). However, some structural differences were detected between Cac1C and typical WHDs. Cac1C lacked one β-strand and the w2 loop, while contained an additional α-helix at the C-terminal compared with canonical WHDs (Supplementary Figure S1C and D).

WHD is a versatile and widespread structural element, usually involved in nucleic acid binding. Its diverse functions range from transcription factor sequence recognition to bulldozer-like strand-separating wedges in helicases to mediate protein–protein interactions (45). The electrostatic potential surface of Cac1C highlighted a positively charged cavity, suggesting that this domain may be also involved in nucleic acid binding (Figure 1D). Eight positively charged residues (Lys553, Lys560, Lys564, Lys568, Arg573, Lys577, Arg582 and Lys583) from α2, α3 and w1 constituted the positively charged surface (Figure 1A and D).

The Cac1C positively charged surface is responsible for DNA binding

The WHD structure and the positively charged cavity on the Cac1C surface suggest that Cac1C is involved in DNA binding. To test this idea, we performed EMSA assays and found that the recombinant Cac1C protein bound to dsDNA of
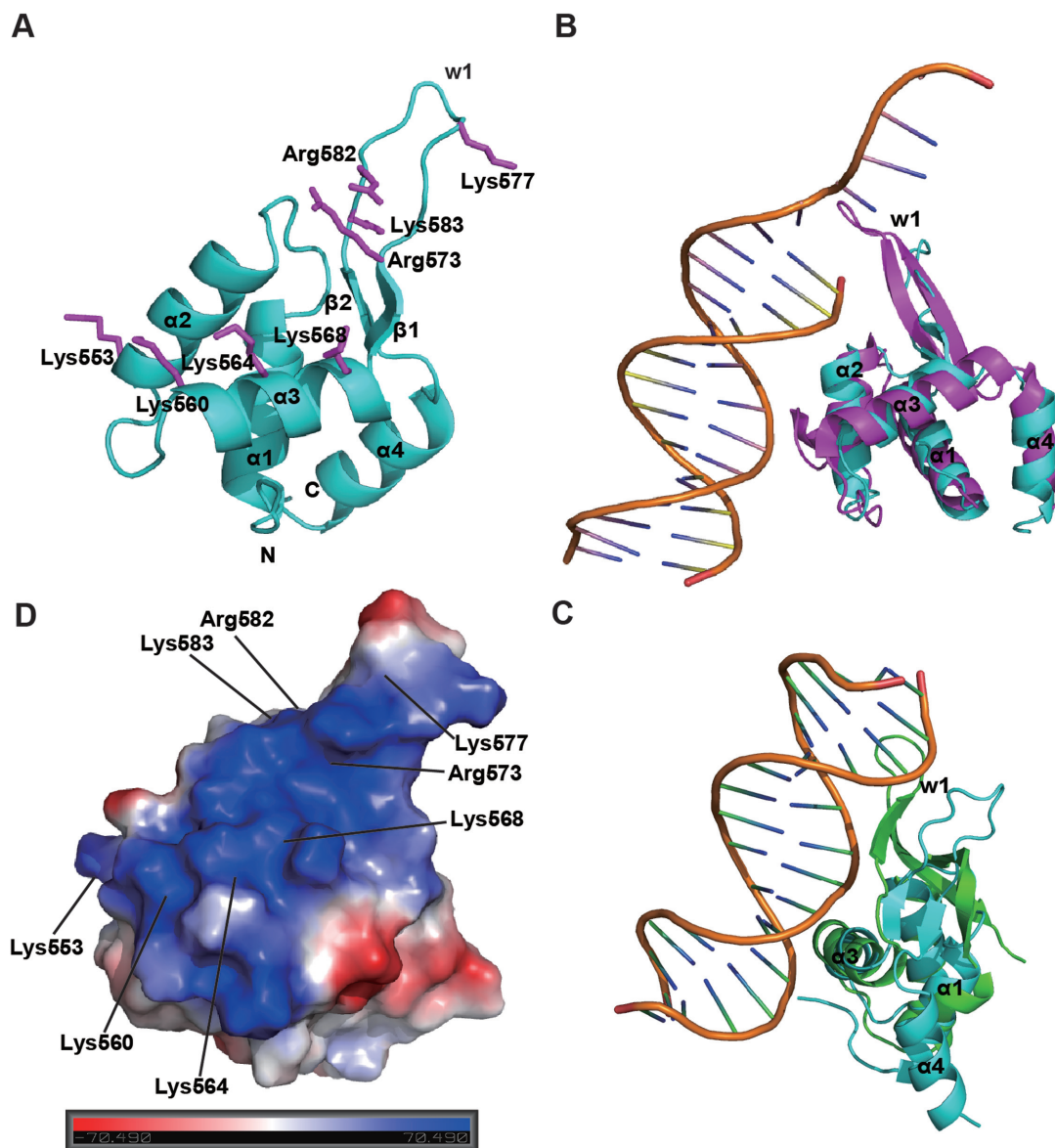
Figure 1. Structure of Cac1C. (**A**) A overview of Cac1C. Key residues predicted to be involved in DNA binding are shown as stick representations (magentas). Secondary structure elements of Cac1C are labeled. (**B** and **C**) Structural comparison of Cac1C (cyan) with RECQ1 (magenta PDB 2WWY, panel B) and RFX1 (green PDB 1DP7, panel C). All α helices and w1 are labeled. The root mean square deviations (RMSD) of these two structures with Cac1C are 2.60 Å and 2.15 Å, respectively. (**D**) The electrostatic potential surface of Cac1C shows a positively charged region composed by eight basic residues. The positively charged, negatively charged and neutral regions are shown in blue, red and white, respectively.

different lengths (10–16 bp) and different sequences (AT-rich or GC-rich) as well as ssDNA *in vitro* (Supplementary Figure S2A and B). Cac1C DNA binding was further validated by a DNA-protein binding assay using streptavidin Sepharose beads coupled with 58 bp DNA (Supplementary Figure S3).

To further determine the detailed mechanism of the interaction between Cac1C and dsDNA, we mutated eight basic residues (lysine or arginine) in the positively charged cavity to glutamic acid respectively, and examined their DNA-binding abilities. Mutations in five residues (K560E, K564E, K568E, R573E and R582E), located in α3 and w1, significantly reduced or impaired Cac1 DNA-binding abil-

ity compared with WT Cac1C (Figure 2A and B), without apparent effects on the overall structure of Cac1C as examined by CD analysis (Supplementary Figure S4). Mutations in the other three residues (K553E, K577E and K583E) had no apparent effect on Cac1C DNA-binding ability (Figure 2A and B). We noticed that the side chains of these residues extended to the outside of the DNA-binding surface (Figure 1A). These results indicate that Cac1C interacts with DNA mainly through α3 and w1. Thus, Cac1C may bind DNA in similar way as WHD-containing proteins RFX1 (Figure 1D) and E2F4 (Supplementary Figure S1A), in which both α3 and w1 interact with DNAs. In the WHD of transcription factors, α3 has been identified as the
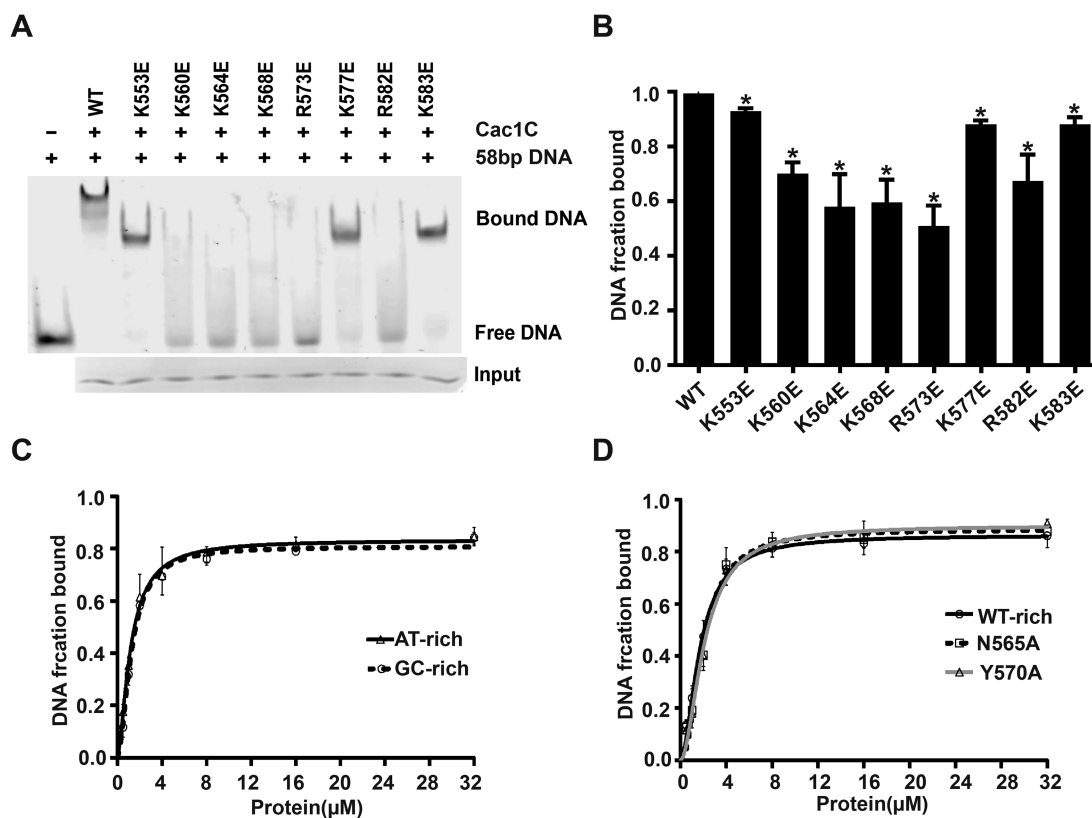
Figure 2. The DNA-binding ability of Cac1C assessed by EMSA. (**A**) The DNA-binding ability of Cac1C was reduced by mutations at charged residues locating on the positively charged surface. A total of 5 μM of 58 bp FAM labeled DNA was incubated with 20 μM WT Cac1C or different Cac1C mutant proteins and analyzed in 4% native PAGE. The gels were scanned with Typhoon Troi + (GE Healthcare). (**B**) Quantification of DNA binding of WT and each mutant in panel A. The integrated density value of each band was quantified by ImageJ and normalized against WT proteins. Error bars indicate the average and SD of three independent experiments calculated by Student's *t*-test. *$P < 0.05$ compared to WT. (**C**) Cac1C showed similar binding affinity to AT-rich and GC-rich DNA. (**D**) Mutations N565A and Y570A had no apparent effect on the DNA-binding ability of Cac1C. The results of panel C and D came from analyzing of data shown in Supplementary Figure S5.

key helix that makes specific polar or hydrophobic contacts with dsDNA sequences through the side chains of special residues, including tyrosine, asparagine, arginine and histidine (43,46,47). However, we observed that Cac1C did not have selectivity for DNA sequence (Figure 2C and Supplementary Figure S5A). Consistent with these results, mutations at the asparagine and tyrosine residues on the α3 of Cac1C (N565A and Y570A) did not affect the Cac1C binding affinity to dsDNA (Figure 2D and Supplementary Figure S5B). Furthermore, the replacement of lysine with arginine (or arginine with lysine) at the eight positively charged residues also did not affect the Cac1C DNA binding ability (Supplementary Figure S6). Thus, we propose that Cac1C binds to various DNAs through electronic interactions between its positively charged residues and the DNA phosphate group.

Cac1C bound to dsDNA with a dissociation constant Kd of ∼2 μM based on EMSA assays (Supplementary Figure S5B). The Cac1C binding affinity to dsDNA was in a range similar to some WHD-containing proteins, such as Ash2L (Kd = 12 μM) (48), transcription factor FoxM1 (Kd = 7 μM) (49) and the histone chaperone Rtt106 (Kd > 20 μM) (50), suggesting that the DNA-binding ability is important for CAF-1's function.

Cac1C contributes to CAF-1-DNA interaction

Cac1 is a subunit of the CAF-1 complex consisting of Cac1, Cac2 and Cac3. To test whether Cac1C contributes to DNA binding of the CAF-1 complex, we used streptavidin Sepharose beads labeled with 58 bp DNA to pulldown the GST-tagged CAF-1 (Cac1, GST-Cac2 and Cac3) or the mutated complex (Supplementary Figure S7). GST-Cac2 in the CAF-1 complex was pulled down by DNA, whereas GST-Cac2 alone was not, suggesting that the CAF-1 complex binds to dsDNA *in vitro* (Figure 3A). Furthermore, mutations in the basic residues, K564E/K568E and R582E/K583E resulted in a significant reduction in the amount of pulled down CAF-1 complex (Figure 3A). These mutations did not affect the formation of CAF-1 complex (Supplementary Figure S8). Because these two mutations almost abolished Cac1C-DNA interaction (Supplementary Figure S3), but not the CAF-1-DNA interaction (Figure 3A), Cac1C may be one of the domains that contribute to the interaction between CAF-1 and DNA.
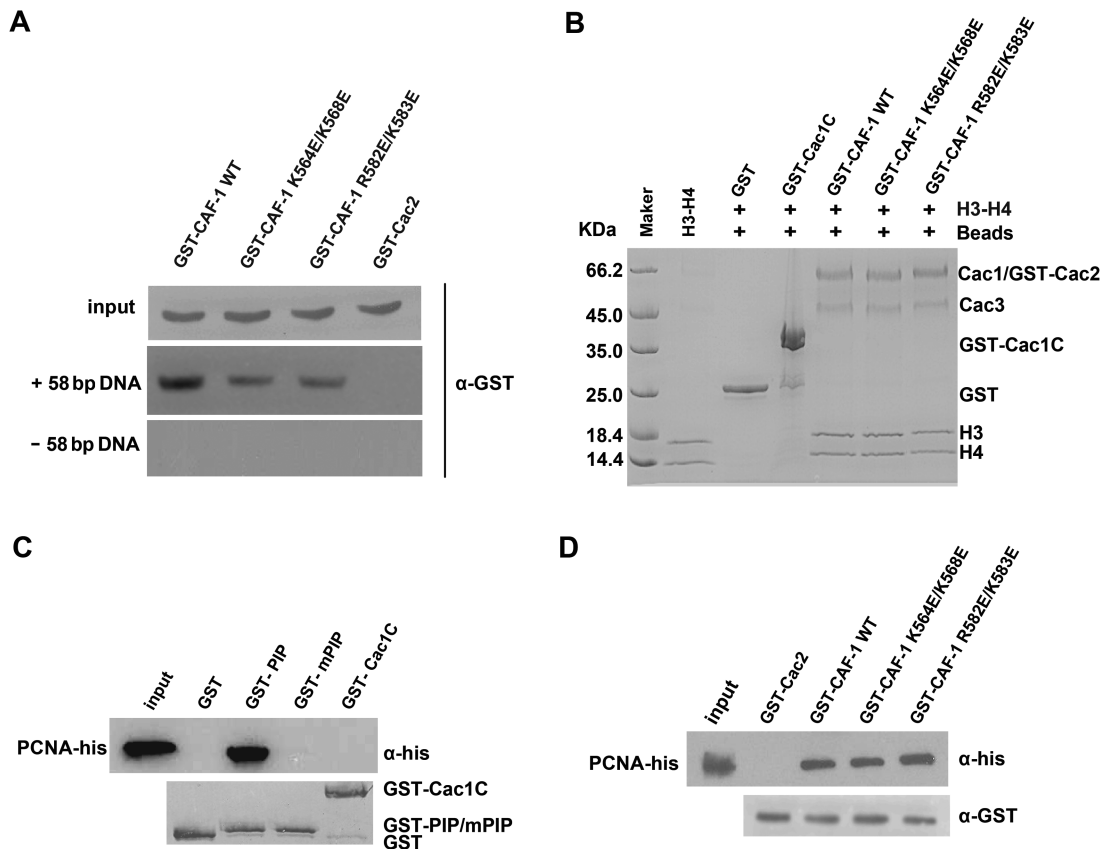
Figure 3. Cac1C contributes to the interaction between CAF-1 and DNA, and DNA-binding mutations have no apparent effect on the ability of CAF-1 to bind its partners. (**A**) Cac1C was involved in the interaction between CAF-1 and DNA. Equal amounts of streptavidin sepharose beads labeled with 58 bp DNA were used to pull down WT or mutated CAF-1 complex (Cac1, GST-Cac2 and Cac3). Pull-downed proteins were detected by immunoblotting with antibodies against GST. Compared with WT, two CAF-1 mutants, K564E/K568E and R582E/K583E, showed reduced DNA-binding abilities. GST-tagged Cac2 alone was used as a negative control. (**B**) Cac1C does not contribute to the interaction between CAF-1 and H3–H4. GST-Cac1C, WT and mutated GST-CAF-1 complexes (Cac1, GST-Cac2, Cac3) were used to pull down histone H3–H4 at 300 mM NaCl. Pulled-down proteins were detected by Coomassie Blue staining. Note that Cac1 and GST-Cac2 were at the similar position in the SDS-PAGE gel (Supplementary Figure S7). (**C**) Cac1C does not interact with PCNA *in vitro*. GST-Cac1 PIP domain, GST-Cac1 PIP mutant (F233A/F234A, GST-mPIP) and GST-Cac1C were used to pull down recombinant his-tagged PCNA. PCNA was detected by immunoblotting with antibodies against his. GST tagged proteins were detected by Coomassie Blue staining. GST was use as negative control. (**D**) CAF-1 mutants defective in DNA binding do not affect the CAF-1-PCNA interaction *in vitro*. The experiments were performed as described above except that GST-Cac2 (negative control) and WT or mutated GST-CAF-1 complex were used in the experiments.

Cac1C mutations that disrupt DNA interaction have no apparent effect on the ability of CAF-1 to bind its partners

CAF-1 is a histone H3–H4 chaperone that binds and deposits histone (H3–H4)$_2$ tetramers onto replicating DNA (6,10). In addition, CAF-1 is recruited to DNA replication forks, in part, through its interaction with PCNA (26–29). Therefore, we analyzed how K564E/K568E and R582E/K583E mutations affected the ability of CAF-1 to form complex and interact with H3–H4 and PCNA. To evaluate whether Cac1C participated in histone binding, we performed a histone-binding assay using GST-tagged proteins and recombinant histone H3–H4 at different salt concentrations. The results showed that Cac1C did not directly bind histone H3–H4 *in vitro* (Figure 3B and Supplementary Figure S9). However, the CAF-1 complex bound H3–H4 under the same conditions. Importantly, mutations K564E/K568E and R582E/K583E did not affect the formation of the CAF-1 complex (Supplementary Figure S8) as well as the ability of this complex to bind H3–H4 (Figure

3B). Similarly, Cac1C did not bind PCNA (Figure 3C), and these two mutations did not affect the ability of CAF-1 to bind PCNA *in vitro* (Figure 3D). These results suggest that the DNA-binding ability of CAF-1 through the Cac1C domain is independent of its ability to bind histone or PCNA *in vitro*.

Disruption of Cac1C DNA-binding ability partially affects CAF-1's function in *HMR* silencing and response to DNA damaging agents

It is known that cells lacking CAF-1 exhibit defects in transcriptional silencing (51,52). In budding yeast, three loci: telomeres, silent mating-type loci and rDNA repeats form silent chromatin. The silencing depends on structural proteins, such as the silent information regulatory proteins. It has been shown that *cac1Δ rtt106Δ* mutant cells exhibit silencing defects at telomeres and the *HMR* silent mating-type locus (38). To determine whether Cac1C DNA-binding

ability was important for CAF-1's function *in vivo*, we performed the GFP-based *HMR* silencing assay to evaluate the effect of Cac1C DNA-binding mutations on transcriptional silencing at the *HMR* locus. In this assay, the GFP transgene inserted at the *HMR* locus was silenced in WT cells. Consistent with previous results, ∼60% of *cac1Δ rtt106Δ* mutant cells expressed GFP, which could be rescued by expressing WT Cac1 ([38]) (Figure [4]A). In contrast, Cac1 mutants defective in DNA binding, while expressed at a level similar or close to that of WT Cac1 (Supplementary Figures S10 and S11), only partially rescued the *HMR* silencing defects, with mutations at multiple charged residues exhibiting larger effects than single-site mutations (Figure [4]A), suggesting that Cac1C DNA-binding ability is important for the role of CAF-1 in transcriptional silencing.

Cac1Δ rtt106Δ mutant cells are sensitive to DNA damaging agents, such as camptothecin (CPT)([40]). Therefore, we also tested how cells expressing Cac1 DNA-binding defective mutants affected the response to this DNA damaging agent. Similarly, cells expressing the Cac1 mutants defective in DNA binding grew slower in media containing CPT than those expressing WT Cac1 (Figure [4]B). These results suggest that Cac1C DNA-binding activity is important for CAF-1's function in response to DNA damaging agents.

Cac1C DNA-binding ability is synergistic with Cac1-PCNA interaction

Compared with *cac1Δ rtt106Δ* mutant cells, we observed only partial defects in *HMR* silencing and response to DNA damaging agents in cells expressing a *cac1* mutant defective in DNA binding. Several studies have shown that the interaction between CAF-1 and PCNA is important for CAF-1's role in nucleosome assembly ([26–29]). Therefore, we tested whether Cac1C DNA-binding activity was synergistic with Cac1-PCNA interaction. Cells expressing Cac1 mutant with mutations at the PCNA interaction peptides (PIP) motif also exhibited partial defects in *HMR* silencing and DNA damage sensitivity assays (Figure [4]A and C). Remarkably, when the PIP mutation was combined with each of the three *cac1* mutations defective in DNA binding, the combined mutants exhibited defects in silencing and DNA damage response similar to *cac1Δ* mutation (Figure [4]A and C). These results suggest that Cac1C DNA-binding activity has a synergistic role with Cac1-PCNA interaction during transcriptional silencing and in response to DNA damaging agent.

Cac1C is dispensable for PCNA binding and K564E/K568E and R582E/K583E mutations have no apparent effect on PCNA binding *in vitro* (Figure [3]C and D). To understand the synergistic effect between Cac1-PCNA and Cac1-DNA interactions, we determined how the K564E/K568E and R582E/K583E mutations affected complex formation and PCNA binding in the cells. In brief, Cac2-TAP was purified from yeast cells expressing WT Cac1 or Cac1 mutants (K564E/K568E and R582E/K583). As shown in Supplementary Figure S11, similar quantities of WT or mutated Cac1 were co-purified with Cac2, consistent with the *in vitro* results that these mutations do not affect Cac1–Cac2 interaction. Interestingly, the PCNA-Cac1 interaction decreased signif-

icantly in K564E/K568E and R582E/K583E mutant cells, suggesting that the ability of Cac1 to bind DNA is important for its interaction with PCNA at replication forks in cells (see Discussion). Furthermore, cells expressing Cac1 mutants (K564E/K568E and R582E/K583E) alone or in combination with the PIP mutation did not affect cell cycle progression (Supplementary Figure S12A). Finally, using a chromatin binding assay ([39]), we observed that the Cac1 PIP mutant bound to chromatin as efficiently as WT Cac1, whereas mutations K564E/K568E and R582E/K583E led to a marked reduction in the association of Cac1 with chromatin compared to WT Cac1 (Supplementary Figure S12B). Thus Cac1C DNA-binding activity is also important for chromatin binding by Cac1 in budding yeast cells.

The p150 DNA-binding WHD is important for its localization at replication foci

CAF-1 is conserved in all eukaryotic cells. A C-terminal region with sequence similarity to Cac1C could be detected in both human p150 (Hsp150C, residues 727–854 aa) and mouse p150 (Mmp150C, residues 706–827 aa) (Supplementary Figure S13). Using HHpred (http://toolkit.tuebingen.mpg.de/hhpred), we also found that both Hsp150C and Mmp150C showed sequences homology to the DNA-binding domain (DBD) of human general transcription factor IIF subunit 2 (GTF2F2) (Supplementary Figure S14A). GTF2F2 DBD folds into WHD motifs (Supplementary Figure S14B), suggesting that the C-terminal regions of human and mouse p150 form a WHD motif. A structural prediction (SWISS-MODEL, http://swissmodel.expasy.org/) showed that the Hsp150C structure was folded into a WHD motif (Supplementary Figure S14C). Therefore, we determined whether Hsp150C and Mmp150C bound DNA using EMSA. Both Hsp150C and Mmp150C bound to dsDNA *in vitro* (Supplementary Figure S15). Importantly, mutations in the four positively charged residues (4K) located at the predicted α3 helix of the WHD motif, which was involved in Cac1C DNA binding, abolished their abilities to bind DNA (Supplementary Figure S15). These results suggest that both human and mouse p150 contain a DNA binding WHD motif.

Thereafter, we asked how mutations at the p150 DNA binding domain affect CAF-1 localization at replication foci. To do this, we expressed GFP-tagged WT or mutated mouse p150 in NIH3T3 cells and determined their localization by fluorescence microscopy. It is known that there are two PIP motifs responsible for PCNA interaction in p150, termed as PIP1 and PIP2 ([53]). In addition to PCNA, p150 also binds to heterochromatin protein 1 (HP1) proteins ([54])(Figure [5]A). Therefore, WT p150 co-localized with PCNA at replication foci, but not heterochromatin foci (DAPI), during early and mid S phase of the cell cycle. In non-S phase cells, GFP-p150 was localized with DAPI foci (Figure [5]A). It has been reported that p150 PIP deletion mutants exhibit partial and full localization defects ([53]) (Figure [5]B). A partial localization defect refers to the fact that GFP-p150 PIP mutants co-localize with both replication foci (PCNA) and heterochromatic foci during early and mid S phase in a fraction of cells. It is believed that
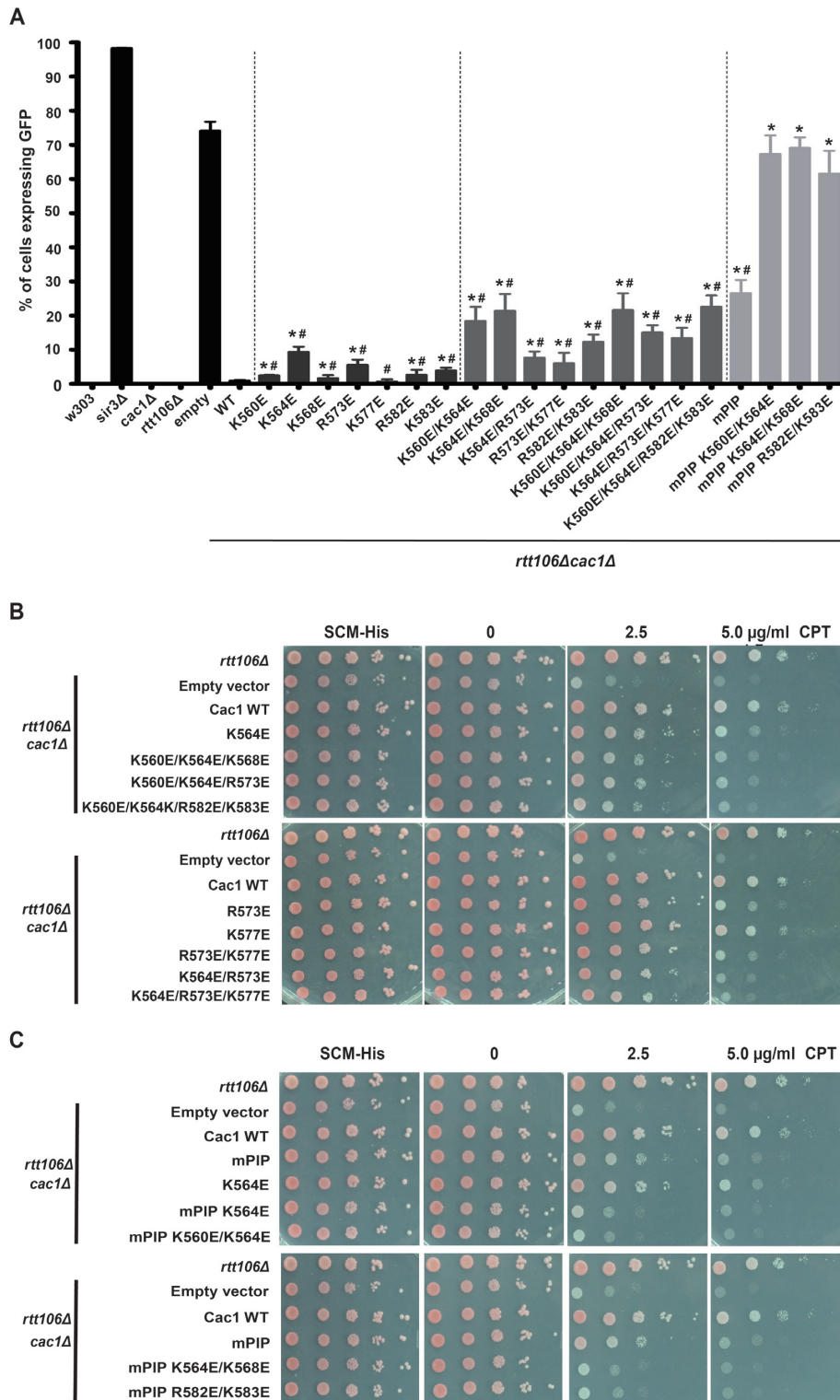
Figure 4. The Cac1C-DNA interaction and the Cac1-PCNA interaction function in parallel to mediate Cac1's role in *HMR* silencing and response to DNA damage. (**A** and **B**) Cells harboring Cac1 DNA binding mutant exhibit defects in transcriptional silencing at the *HMR* locus (A) as well as increased sensitivity toward DNA damaging agent CPT (B). Cells with indicated genotypes were analyzed for GFP expression using FACS. The W303 cells (less than 1%) and cells with *sir3Δ* (over 95%) were used as standards for GFP expression. Error bars indicate SEM analysis of at least three independent experiments. (**B**) The sensitivity to DNA damage was analyzed through a 10-fold serial dilution of cells of indicated genotype onto regular growth media (SCM-His) or media with CPT. (**A** and **C**) Cells expressing Cac1 mutants harboring mutations at both DNA-binding domain and PCNA binding motif showed an synthetic defects in *HMR* silencing (A) and response to CPT (C). The experiments were repeated at least three times and Student's *t*-test was used to calculate *P*-value. *$P < 0.05$ compared to WT, #$P < 0.05$ compared to empty vector. The expression of the WT and mutated Cac1 is shown in Supplementary Figure S10.
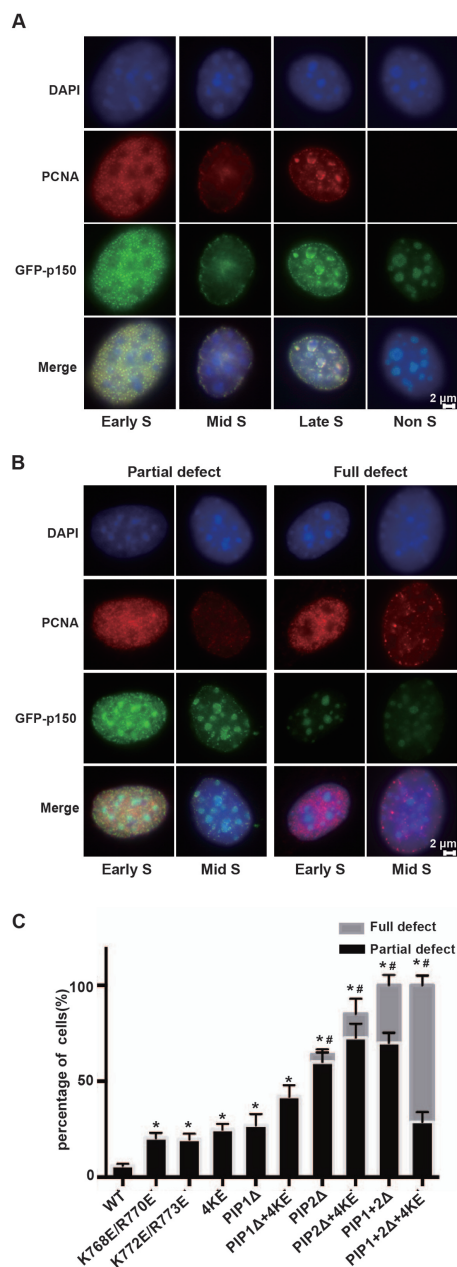
Figure 5. Mutations at mouse p150 DNA-binding domain resulted in mis-localization at replication foci. (**A**) Representative images of WT GFP-p150, PCNA and DAPI staining in early, middle and late S phase and non-S phase cells. GFP-tagged WT p150 was expressed in mouse NIH3T3 cells using lentivirus-based system. GFP and PCNA were stained with monoclonal antibodies. DAPI staining was used to mark foci of pericentric heterochromatin. PCNA does not bind to chromatin in non-S phase cells and the soluble PCNA will be washed away after pre-extraction and therefore little PCNA IF signals (black) were detected in non-S phase cells. (**B**) Representative images of mutant GFP-p150 showing partial- and full-localization defects. In cells exhibiting partial-localization defect, GFP-p150 co-localized with both PCNA and heterochromatin foci (DAPI), while all the GFP-p150 mis-targeted to heterochromatin foci in cells exhibiting full-localization defect cells during S phase. PCNA staining was used to mark S phase cells. (**C**) Analysis of the percentage of cells showing partial- and full-localization defects. Error bars indicate standard error of mean (SEM) of at least three experiments calculated by Student's *t*-test. *$P < 0.05$ partial defect compared to WT, #$P < 0.05$ full defect compared to WT. The expression of the WT and mutated p150 is shown in Supplementary Figure S16.

GFP-p150 PIP mutants form dimmers with endogenous p150, which is responsible for the partial defect observed in PIP mutant cells (53). In contrast, the GFP-p150 mutant was mis-targeted to heterochromatin foci and did not co-localize with PCNA during early and mid S phase in cells with a full defect.

We observed that cells expressing the p150 DNA binding mutant (4KE) exhibited an increase in the percentage of cells with a partial defect compared with that of WT p150 (Figure 5C). In addition, when the DNA binding mutation (4KE) was combined with deletion of two PIP motifs (PIP1 + 2Δ), the percentage of cells with the full CAF-1 p150 localization defect increased significantly compared with the p150 mutant lacking both PIP1 and PIP2 (Figure 5C). All CAF-1 p150 mutants were expressed to a similar level to that of WT CAF-1 p150 (Supplementary Figure S16). These results indicate that the ability of mouse p150 to bind DNA, together with its ability to bind PCNA, is important for its localization at replication foci.

DISCUSSION

CAF-1 contains a DNA-binding WHD at its C terminus

Histone chaperones are a group of proteins that deliver histones to DNA for nucleosome assembly and/or receive histones from disassembled nucleosomes. CAF-1 is a classic histone H3–H4 chaperone involved in DNA replication-coupled nucleosome assembly. Our results reveal that yeast CAF-1 also interacts with DNA directly *in vitro* and its ability to bind DNA is likely conserved in eukaryotic cells. In addition, we show that the DNA-binding domain, Cac1C, forms a WHD structure. WHD is a versatile nucleic-acid-binding structural element, and a large number of WHD-containing proteins with diverse biological functions have been characterized (45). For instance, many transcription factors use WHD domains for sequence-specific DNA recognition. In addition, some helicases involved in DNA recombination and repair utilize WHD domains as a strand-separating wedge. Finally, some WHDs mediate protein–protein interactions. Cac1C is the first WHD-containing protein discovered in histone chaperones. While our results suggest that Cac1C is similar, in many ways, to the WHDs found in transcription factors. However, the WHD domain in Cac1C does not have a DNA sequence preference and does not utilize specific residues found in transcription factors for sequencing recognition (Figure 2). We suggest that this property enables CAF-1 to bind to replicated or repaired DNA, rather than some specific DNA elements.

Two histone chaperones, yeast Rtt106 (50) and human NAP-1 family member SET (55), have been reported previously to possess DNA-binding ability. Both SET and Rtt106 use overlapping surfaces to bind histones and DNA. In contrast, Cac1C appears to be involved specifically in DNA binding but not in protein–protein interactions, including CAF-1-histone and CAF-1-PCNA interactions. Therefore, it is possible that Cac1C-DNA interaction regulates CAF-1's role in nucleosome assembly and other processes distinctly from the Rtt106 and SET DNA-binding regions.
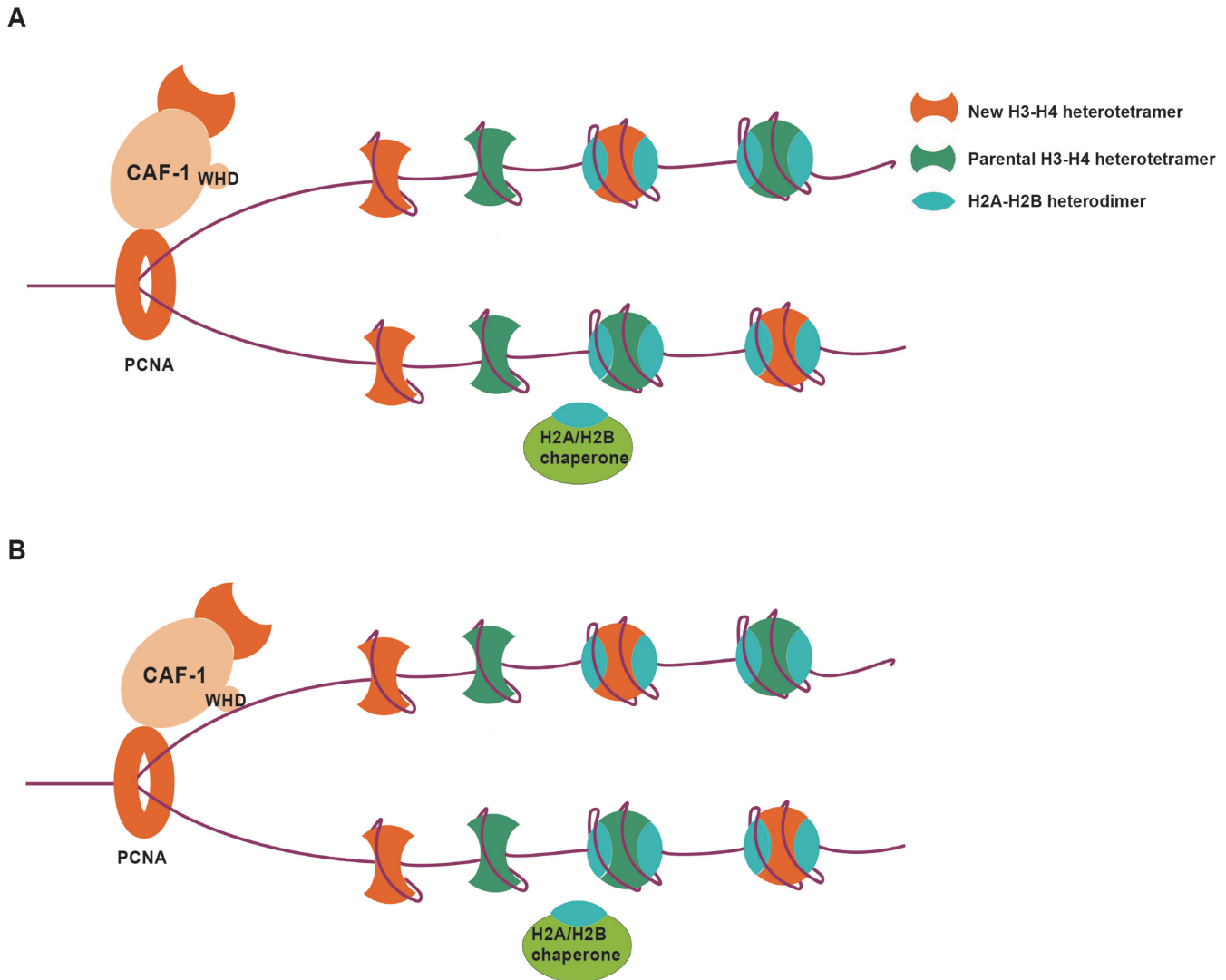
Figure 6. A model for the WHD–DNA interaction in stabilizing CAF-1 at replication forks. (**A**) CAF-1 is recruited to replication forks through its interaction with PCNA. (**B**) After recruited, CAF-1 binds to DNA in close proximity through its WHD, thereby stably associating with replication forks.

The DNA-binding WHD of CAF-1 stabilizes CAF-1 at replication forks

We provide the following lines of evidence supporting the idea that the ability of the CAF-1 WHD motif to bind DNA is involved in recruitment and/or stabilization of CAF-1 at replication forks. First, we show that in budding yeast, Cac1 mutants defective in DNA binding exhibit partial defects in silencing and in response to DNA damaging agents. Remarkably, mutations at both the PCNA and DNA binding sites of Cac1 result in complete loss of Cac1 function in gene silencing and maintenance of genome stability (Figure 4). Remarkably, disrupting Cac1C DNA binding affects CAF-1-PCNA interactions *in vivo* (Supplementary Figure S11). However, Cac1C does not bind PCNA *in vitro*, and the same mutations in Cac1C do not affect CAF-1-PCNA interaction (Figure 3). At replication forks, PCNA forms a homotrimer and encircles replicating DNA. While it is possible that Cac1C DNA binding mutations may affect the interactions between Cac1 and other components of PCNA

foci, we suggest that Cac1C binds to DNAs encircled by PCNA, which, in turn, stabilizes CAF-1-PCNA interaction at replication forks. This interpretation is supported by our studies in mammalian cells. We show that while mutations compromising mouse p150 to bind DNA result in partial defect in localization at replication foci, p150 mutants, harboring both mutations at PIPs and DNA-binding domain, mis-target to heterochromatin in early and mid S phase cells (Figure 5). Therefore, both p150 DNA-binding activity and p150-PCNA interaction are important for the association of p150 with DNA replication foci. Based on our studies, we propose the following working model on how Cac1C contributes to the localization of CAF-1 at replication forks. First, CAF-1 is recruited to DNA replication forks through its interaction with PCNA (Figure 6A). Once recruited, the Cac1C-DNA interaction stabilizes CAF-1 at replication forks for nucleosome assembly (Figure 6B). In addition to stabilizing CAF-1 at replication forks, it is possible that the Cac1C-DNA interaction may signal the CAF-1 complex

to release H3–H4 from CAF-1 to replicating DNA. While the latter possibility is speculative in nature, it is largely unknown how CAF-1 is relieved from binding to H3–H4 for nucleosome assembly. CAF-1 is also known to interact with HP1 (54). Therefore, it is possible that CAF-1-DNA interaction may have other functions other than nucleosome assembly. Future studies are needed to test these models.

In summary, our studies support a working model whereby the C-terminal DNA-binding domain and the PIP domain of Cac1/p150 function together to recruit and stabilize CAF-1 at replication forks, most likely for nucleosome assembly. It is known that nucleosome assembly pathway can be regulated in different ways, including histone modification and CAF-1 dimerization. Our structural, biochemical and functional studies of the Cac1C DNA-binding domain yield additional layers of regulation of CAF-1 in nucleosome assembly.

ACCESSION NUMBER

Coordinates have been deposited in the RCSB Protein Data Bank PDB: 5EJO.

SUPPLEMENTARY DATA

Supplementary Data are available at NAR Online.

ACKNOWLEDGEMENT

FUNDING

REFERENCES

1. Moazed,D. (2011) Mechanisms for the inheritance of chromatin states. *Cell*, **146**, 510–518.
2. Luger,K., Mader,A.W., Richmond,R.K., Sargent,D.F. and Richmond,T.J. (1997) Crystal structure of the nucleosome core particle at 2.8 A resolution. *Nature*, **389**, 251–260.
3. Davey,C.A., Sargent,D.F., Luger,K., Maeder,A.W. and Richmond,T.J. (2002) Solvent mediated interactions in the structure of the nucleosome core particle at 1.9 a resolution. *J. Mol. Biol.*, **319**, 1097–1113.
4. Vasudevan,D., Chua,E.Y. and Davey,C.A. (2010) Crystal structures of nucleosome core particles containing the '601' strong positioning sequence. *J. Mol. Biol.*, **403**, 1–10.
5. Falbo,K.B. and Shen,X. (2006) Chromatin remodeling in DNA replication. *J. Cell. Biochem.*, **97**, 684–689.
6. Groth,A., Rocha,W., Verreault,A. and Almouzni,G. (2007) Chromatin challenges during DNA replication and repair. *Cell*, **128**, 721–733.
7. Verreault,A. (2000) De novo nucleosome assembly: new pieces in an old puzzle. *Genes Dev.*, **14**, 1430–1438.
8. Krude,T. and Keller,C. (2001) Chromatin assembly during S phase: contributions from histone deposition, DNA replication and the cell division cycle. *Cell. Mol. Life Sci.*, **58**, 665–672.
9. Tyler,J.K. (2002) Chromatin assembly. Cooperation between histone chaperones and ATP-dependent nucleosome remodeling machines. *Eur. J. Biochem.*, **269**, 2268–2274.
10. Smith,S. and Stillman,B. (1989) Purification and characterization of CAF-I, a human cell factor required for chromatin assembly during DNA replication in vitro. *Cell*, **58**, 15–25.
11. Quivy,J.P., Gerard,A., Cook,A.J., Roche,D. and Almouzni,G. (2008) The HP1-p150/CAF-1 interaction is required for pericentric heterochromatin replication and S-phase progression in mouse cells. *Nat. Struct. Mol. Biol.*, **15**, 972–979.
12. Polo,S.E., Roche,D. and Almouzni,G. (2006) New histone incorporation marks sites of UV repair in human cells. *Cell*, **127**, 481–493.
13. Ye,X., Franco,A.A., Santos,H., Nelson,D.M., Kaufman,P.D. and Adams,P.D. (2003) Defective S phase chromatin assembly causes DNA damage, activation of the S phase checkpoint, and S phase arrest. *Mol. Cell*, **11**, 341–351.
14. Baldeyron,C., Soria,G., Roche,D., Cook,A.J. and Almouzni,G. (2011) HP1alpha recruitment to DNA damage by p150CAF-1 promotes homologous recombination repair. *J. Cell Biol.*, **193**, 81–95.
15. Quivy,J.P., Roche,D., Kirschner,D., Tagami,H., Nakatani,Y. and Almouzni,G. (2004) A CAF-1 dependent pool of HP1 during heterochromatin duplication. *EMBO J.*, **23**, 3516–3526.
16. Adam,S., Polo,S.E. and Almouzni,G. (2013) Transcription recovery after DNA damage requires chromatin priming by the H3.3 histone chaperone HIRA. *Cell*, **155**, 94–106.
17. Nakano,S., Stillman,B. and Horvitz,H.R. (2011) Replication-coupled chromatin assembly generates a neuronal bilateral asymmetry in C. elegans. *Cell*, **147**, 1525–1536.
18. Yu,Z., Wu,H., Chen,H., Wang,R., Liang,X., Liu,J., Li,C., Deng,W.M. and Jiao,R. (2013) CAF-1 promotes Notch signaling through epigenetic control of target gene expression during Drosophila development. *Development*, **140**, 3635–3644.
19. Huang,H., Yu,Z., Zhang,S., Liang,X., Chen,J., Li,C., Ma,J. and Jiao,R. (2010) Drosophila CAF-1 regulates HP1-mediated epigenetic silencing and pericentric heterochromatin stability. *J. Cell Sci.*, **123**, 2853–2861.
20. Zeng,A., Li,Y.Q., Wang,C., Han,X.S., Li,G., Wang,J.Y., Li,D.S., Qin,Y.W., Shi,Y., Brewer,G. *et al.* (2013) Heterochromatin protein 1 promotes self-renewal and triggers regenerative proliferation in adult stem cells. *J. Cell Biol.*, **201**, 409–425.
21. Han,J., Zhou,H., Li,Z., Xu,R.M. and Zhang,Z. (2007) The Rtt109-Vps75 histone acetyltransferase complex acetylates non-nucleosomal histone H3. *J. Biol. Chem.*, **282**, 14158–14164.
22. Han,J., Zhang,H., Wang,Z., Zhou,H. and Zhang,Z. (2013) A Cul4 E3 ubiquitin ligase regulates histone hand-off during nucleosome assembly. *Cell*, **155**, 817–829.
23. Liu,W.H., Roemer,S.C., Port,A.M. and Churchill,M.E. (2012) CAF-1-induced oligomerization of histones H3/H4 and mutually exclusive interactions with Asf1 guide H3/H4 transitions among histone chaperones and DNA. *Nucleic Acids Res.*, **40**, 11229–11239.
24. Winkler,D.D., Zhou,H., Dar,M.A., Zhang,Z. and Luger,K. (2012) Yeast CAF-1 assembles histone (H3-H4)2 tetramers prior to DNA deposition. *Nucleic Acids Res.*, **40**, 10139–10149.
25. Fazly,A., Li,Q., Hu,Q., Mer,G., Horazdovsky,B. and Zhang,Z. (2012) Histone chaperone Rtt106 promotes nucleosome formation using (H3-H4)2 tetramers. *J. Biol. Chem.*, **287**, 10753–10760.
26. Krawitz,D.C., Kama,T. and Kaufman,P.D. (2002) Chromatin assembly factor I mutants defective for PCNA binding require Asf1/Hir proteins for silencing. *Mol. Cell. Biol.*, **22**, 614–625.
27. Moggs,J.G., Grandi,P., Quivy,J.P., Jonsson,Z.O., Hubscher,U., Becker,P.B. and Almouzni,G. (2000) A CAF-1-PCNA-mediated chromatin assembly pathway triggered by sensing DNA damage. *Mol. Cell. Biol.*, **20**, 1206–1218.

28. Shibahara,K. and Stillman,B. (1999) Replication-dependent marking of DNA by PCNA facilitates CAF-1-coupled inheritance of chromatin. *Cell*, **96**, 575–585.

29. Zhang,Z., Shibahara,K. and Stillman,B. (2000) PCNA connects DNA replication to epigenetic inheritance in yeast. *Nature*, **408**, 221–225.

30. Sharp,J.A., Fouts,E.T., Krawitz,D.C. and Kaufman,P.D. (2001) Yeast histone deposition protein Asf1p requires Hir proteins and PCNA for heterochromatic silencing. *Curr. Biol.*, **11**, 463–473.

31. Otwinowski,Z. and Minor,W. (1997) Processing of X-ray diffraction data collected in oscillation mode. *Method Enzymol.*, **276**, 307–326.

32. Sheldrick,G.M. (2008) A short history of SHELX. *Acta Crystallogr. A*, **64**, 112–122.

33. Adams,P.D., Afonine,P.V., Bunkoczi,G., Chen,V.B., Davis,I.W., Echols,N., Headd,J.J., Hung,L.W., Kapral,G.J., Grosse-Kunstleve,R.W. *et al.* (2013) PHENIX: a comprehensive Python-based system for macromolecular structure solution. *Acta Crystallogr. D Biol. Crystallogr.*, **66**, 213–221.

34. Emsley,P., Lohkamp,B., Scott,W.G. and Cowtan,K. (2010) Features and development of Coot. *Acta Crystallogr. D Biol. Crystallogr.*, **66**, 486–501.

35. Vagin,A.A., Steiner,R.A., Lebedev,A.A., Potterton,L., McNicholas,S., Long,F. and Murshudov,G.N. (2004) REFMAC5 dictionary: organization of prior chemical knowledge and guidelines for its use. *Acta Crystallogr. D Biol. Crystallogr.*, **60**, 2184–2195.

36. Laskowski,R.A., Rullmannn,J.A., MacArthur,M.W., Kaptein,R. and Thornton,J.M. (1996) AQUA and PROCHECK-NMR: programs for checking the quality of protein structures solved by NMR. *J. Biomol. NMR*, **8**, 477–486.

37. Dyer,P.N., Edayathumangalam,R.S., White,C.L., Bao,Y., Chakravarthy,S., Muthurajan,U.M. and Luger,K. (2004) Reconstitution of nucleosome core particles from recombinant histones and DNA. *Methods Enzymol.*, **375**, 23–44.

38. Huang,S., Zhou,H., Katzmann,D., Hochstrasser,M., Atanasova,E. and Zhang,Z. (2005) Rtt106p is a histone chaperone involved in heterochromatin-mediated silencing. *Proc. Natl. Acad. Sci. U.S.A.*, **102**, 13410–13415.

39. Liang,C. and Stillman,B. (1997) Persistent initiation of DNA replication and chromatin-bound MCM proteins during the cell cycle in cdc6 mutants. *Genes Dev.*, **11**, 3375–3386.

40. Li,Q., Zhou,H., Wurtele,H., Davies,B., Horazdovsky,B., Verreault,A. and Zhang,Z. (2008) Acetylation of histone H3 lysine 56 regulates replication-coupled nucleosome assembly. *Cell*, **134**, 244–255.

41. Pike,A.C., Shrestha,B., Popuri,V., Burgess-Brown,N., Muzzolini,L., Costantini,S., Vindigni,A. and Gileadi,O. (2009) Structure of the human RECQ1 helicase reveals a putative strand-separation pin. *Proc. Natl. Acad. Sci. U.S.A.*, **106**, 1039–1044.

42. Gajiwala,K.S., Chen,H., Cornille,F., Roques,B.P., Reith,W., Mach,B. and Burley,S.K. (2000) Structure of the winged-helix protein hRFX1 reveals a new mode of DNA binding. *Nature*, **403**, 916–921.

43. Zheng,N., Fraenkel,E., Pabo,C.O. and Pavletich,N.P. (1999) Structural basis of DNA recognition by the heterodimeric cell cycle transcription factor E2F-DP. *Genes Dev.*, **13**, 666–674.

44. Kitano,K., Kim,S.Y. and Hakoshima,T. (2010) Structural basis for DNA strand separation by the unconventional winged-helix domain of RecQ helicase WRN. *Structure*, **18**, 177–187.

45. Harami,G.M., Gyimesi,M. and Kovacs,M. (2013) From keys to bulldozers: expanding roles for winged helix domains in nucleic-acid-binding proteins. *Trends Biochem. Sci.*, **38**, 364–371.

46. Clark,K.L., Halay,E.D., Lai,E. and Burley,S.K. (1993) Co-crystal structure of the HNF-3/fork head DNA-recognition motif resembles histone H5. *Nature*, **364**, 412–420.

47. Ha,S.C., Lokanath,N.K., Van Quyen,D., Wu,C.A., Lowenhaupt,K., Rich,A., Kim,Y.G. and Kim,K.K. (2004) A poxvirus protein forms a complex with left-handed Z-DNA: crystal structure of a Yatapoxvirus Zalpha bound to DNA. *Proc. Natl. Acad. Sci. U.S.A.*, **101**, 14367–14372.

48. Chen,Y., Wan,B., Wang,K.C., Cao,F., Yang,Y., Protacio,A., Dou,Y., Chang,H.Y. and Lei,M. (2011) Crystal structure of the N-terminal region of human Ash2L shows a winged-helix motif involved in DNA binding. *EMBO Rep.*, **12**, 797–803.

49. Littler,D.R., Alvarez-Fernandez,M., Stein,A., Hibbert,R.G., Heidebrecht,T., Aloy,P., Medema,R.H. and Perrakis,A. (2010) Structure of the FoxM1 DNA-recognition domain bound to a promoter sequence. *Nucleic Acids Res.*, **38**, 4527–4538.

50. Liu,Y., Huang,H., Zhou,B.O., Wang,S.S., Hu,Y., Li,X., Liu,J., Zang,J., Niu,L., Wu,J. *et al.* (2009) Structural analysis of Rtt106p reveals a DNA binding role required for heterochromatin silencing. *J. Biol. Chem.*, **285**, 4251–4262.

51. Kaufman,P.D., Kobayashi,R. and Stillman,B. (1997) Ultraviolet radiation sensitivity and reduction of telomeric silencing in Saccharomyces cerevisiae cells lacking chromatin assembly factor-I. *Genes Dev.*, **11**, 345–357.

52. Enomoto,S. and Berman,J. (1998) Chromatin assembly factor I contributes to the maintenance, but not the re-establishment, of silencing at the yeast silent mating loci. *Genes Dev.*, **12**, 219–232.

53. Rolef Ben-Shahar,T., Castillo,A.G., Osborne,M.J., Borden,K.L., Kornblatt,J. and Verreault,A. (2009) Two fundamentally distinct PCNA interaction peptides contribute to chromatin assembly factor 1 function. *Mol. Cell. Biol.*, **29**, 6353–6365.

54. Murzina,N., Verreault,A., Laue,E. and Stillman,B. (1999) Heterochromatin dynamics in mouse cells: interaction between chromatin assembly factor 1 and HP1 proteins. *Mol. Cell*, **4**, 529–540.

55. Muto,S., Senda,M., Akai,Y., Sato,L., Suzuki,T., Nagai,R., Senda,T. and Horikoshi,M. (2007) Relationship between the structure of SET/TAF-Ibeta/INHAT and its histone chaperone activity. *Proc. Natl. Acad. Sci. U.S.A.*, **104**, 4285–4290.